Hybrid Ray-Mode Analysis of E-Polarized Plane Wave Diffraction by a Thick Slit

Hiroshi Shirai, *Senior Member, IEEE*, Masayuki Shimizu, and Ryoichi Sato, *Member, IEEE*

***Abstract*— A high-frequency asymptotic method has been applied to formulate E-polarized plane wave diffraction by a thick slit. The slit structure is regarded as an open-ended parallel plane waveguide cavity, and the excitation of the waveguide modes and their reradiation are derived from a ray-mode conversion technique. Comparison with another method reveals the validity and effectiveness of our formulation.**

***Index Terms*— Geometrical theory of diffraction (GTD), hybrid ray-mode conversion, Poisson summation formula, thick slit.**

I. Introduction

RECENT attention has focused on outdoor-indoor wireless communication through building walls and windows. Typical building walls are made of concrete with iron reinforcing bars, and a canonical problem for this scenario is plane wave diffraction by a thick slit on lossy dielectric walls. As the frequency increases, electromagnetic waves decay more rapidly as they pass through concrete walls. Therefore, the windows on building walls can be considered to be primary gates for such transmitting waves, and a reliable means of estimating the reflection/transmission property through a window that is sufficiently large compared with the wavelength is required. In order to consider the effect of lossy walls, one may compute wall-transmitted rays and compare them with those from a slit aperture.

Diffraction by a slit is a classical problem in electromagnetic diffraction analysis that has been studied in [1]–[4]. For a slit on an infinitely thin conducting screen, an eigenfunction expansion solution in terms of Mathieu functions [1] or the use of the Kobayashi potential (KP) method utilizing Weber-Schafheitlin discontinuous integrals [3], [5] may be possible. These results can be useful references for small apertures.

The diffraction by a wide slit on an infinitely thin screen [2] is easy to formulate since one only needs to consider two edges for the diffraction, and the geometrical theory of diffraction (GTD) [6] may be a powerful tool for such analysis. On the other hand, the diffraction by a thick slit is rather difficult to solve, although it may be analyzed by the KP method [7], [8], the Wiener–Hopf and generalized matrix techniques [9], [10], integral equation approaches [11], [12], and Fourier transform techniques [13], [14]. These previously published studies have mainly dealt with relatively narrow apertures, and few detailed numerical results for scattering patterns have been given for wide apertures.

On the basis of this background, we formulate and analyze the high-frequency diffraction field using asymptotic rays. One may trace all the rays bouncing from the internal walls of a thick slit, but it is impossible to trace all the edge-diffracted multiply reflected rays. Therefore, the solution obtained by summing these bouncing rays would be inaccurate and it would be numerically inefficient to predict the field, particularly in the diffraction region.

A modal description, if available, would be preferable for the internal guiding structure, while a ray description would be preferable for the exterior region [15], [16]. When the internal field can be expressed in terms of the corresponding waveguide modes, formally infinite modal summation may be truncated by propagating modes, or only selected significant modes may be summed to express the field [17], [18]. It would also be much easier to treat some discontinuities inside the waveguide by a scattering matrix approach. Accordingly, to calculate the diffracted field efficiently, each description should be retained in suitable regions. Then, ray-mode conversion between the above two alternative descriptions must be considered at the opening. Since rays and modes are regarded as Fourier transformation pairs, one can utilize the Poisson summation formula to establish an alternative ray or mode description or a hybrid form of both [15] and [17]. Thus, one can construct the solution while maintains the advantages of both descriptions. A similar idea of using ray-mode conversion has already been used to analyze scattering by open cavities such as a trough on the ground [18]–[20].

In the following discussion, we first formulate the diffracted field using the GTD [6]. The ray-mode conversion method [15] is utilized in Section II to obtain the modal excitation and reflection coefficients at the slit aperture. The thus-obtained coefficients are combined through a matrix formulation to synthesize modal reradiation from the aperture. This approach has already been applied successfully to H-polarization by using only dominant edge-diffracted rays [21]. In this paper, we formulate the diffracted field for E-polarization and improve the accuracy of the diffraction field by including multiple edge diffractions and the evanescent modal effect. In Section III, a numerical calculation is performed and a comparison with other solutions validates our analysis. Some concluding remarks are made in Section IV.

Manuscript received January 13, 2016; revised July 27, 2016; accepted September 5, 2016. Date of publication September 13, 2016; date of current version October 27, 2016. This work was supported by JSPS KAKENHI under Grant JP15K06083.

H. Shirai and M. Shimizu are with the Department of Electrical, Electronic and Communication Engineering, Chuo University, Tokyo 112-8551, Japan (e-mail: shirai@ieee.org).

R. Sato is with the Faculty of Education, Niigata University, Niigata 950-2181, Japan.

Color versions of one or more of the figures in this paper are available online at http://ieeexplore.ieee.org.

Digital Object Identifier 10.1109/TAP.2016.2608978

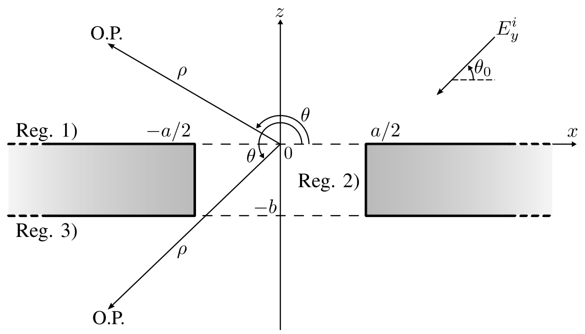

Fig. 1. Geometry of the problem.

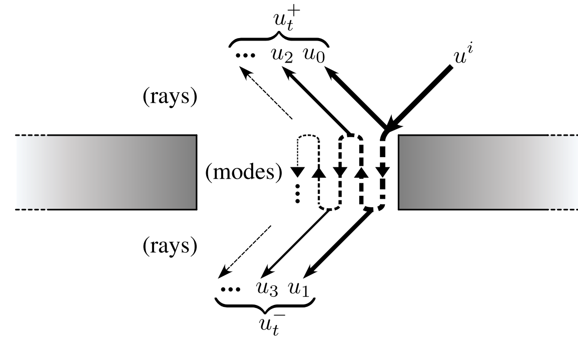

Fig. 2. Schematic of successive excitation of diffracted rays and waveguide modes.

The time-harmonic factor $e^{-i\omega t}$ is assumed and suppressed throughout the text.

II. Formulation

As illustrated in Fig. 1, an E-polarized plane wave expressed as

$$u^i (= E_y^i) = e^{-ik(x\cos\theta_0 + z\sin\theta_0)} \tag{1}$$

illuminates a slit on a thick perfectly conducting screen with incident angle θ_0. The width and thickness of the slit are a and b, respectively, and k is the free space wavenumber. For convenience, the entire region is divided into three regions:

1) a semi-infinite upper half-space ($z > 0$);
2) the slit region ($-b < z < 0$);
3) the lower half-space ($z < -b$).

The slit structure may be considered as an open-ended parallel plane waveguide cavity excited from the outer Reg. 1). One can observe the reflected plane wave

$$u^r = -e^{-ik(x\cos\theta_0 - z\sin\theta_0)} \tag{2}$$

in Reg. 1) and edge-diffracted rays excited at the aperture edges. Let us treat each diffraction component separately.

A. Edge-Diffracted Rays

When an incident plane wave impinges on the edges of the upper aperture ($x = \pm a/2,\ z = 0$), edge-diffracted rays are generated. These primary edge-diffracted rays u_0 give a dominant field in Reg. 1) and a modal excitation in Reg. 2). According to the GTD [6], edge-diffracted rays u_0 can be written for the far field at the observation point ($\rho,\ \theta$) in Reg. 1) as

$$u_0 = u_0^+ + u_0^- \tag{3}$$

$$u_0^+ = C(k\rho) D_{-1}\left(\theta, \theta_0; \frac{3}{2}\pi\right) e^{-ika(\cos\theta + \cos\theta_0)/2} \tag{4}$$

$$u_0^- = C(k\rho) D_{-1}\left(\theta + \frac{\pi}{2}, \theta_0 + \frac{\pi}{2}; \frac{3}{2}\pi\right) \cdot e^{ika(\cos\theta + \cos\theta_0)/2} \tag{5}$$

where $C(\chi)$ is the following asymptotic far-field expression for the 2-D free-space Green's function:

$$C(\chi) = (8\pi\chi)^{-1/2} e^{i(\chi + \pi/4)} \tag{6}$$

and $D_\tau(\phi, \phi_0; \phi_w)$ is Keller's edge diffraction coefficient for a perfectly electric conducting wedge with wedge angle $(2\pi - \phi_w)$ [6]

$$D_\tau(\phi, \phi_0; \phi_w) = \frac{2\pi}{\phi_w} \sin\frac{\pi^2}{\phi_w} \left\{ \left(\cos\frac{\pi^2}{\phi_w} - \cos\frac{\phi - \phi_0}{\phi_w}\right)^{-1} + \tau\left(\cos\frac{\pi^2}{\phi_w} - \cos\frac{\phi + \phi_0}{\phi_w}\right)^{-1} \right\}. \tag{7}$$

An individual edge-diffracted ray, u_0^+ or u_0^-, diverges at the reflection shadow boundary direction $\theta = \pi - \theta_0$. However, their combination $u_0 (= u_0^+ + u_0^-)$ becomes a finite value owing to the cancellation of each diverging feature.

Multiple edge diffractions between the aperture edges occur, and this effect cannot be ignored when the slit aperture becomes narrower. The effect of these multiple edge-diffracted rays can also be formulated by the GTD [2], [22], and the following terms may be added to (3):

$$\begin{aligned} &C(k\rho)\left\{ D_{-1}\left(\pi, \theta_0; \frac{3}{2}\pi\right) D_{-1}\left(\frac{\pi}{2} + \theta, \frac{\pi}{2}; \frac{3}{2}\pi\right) \right. \\ &\quad \cdot e^{ika(\cos\theta - \cos\theta_0)/2} + D_{-1}\left(\frac{\pi}{2}, \frac{\pi}{2} + \theta_0; \frac{3}{2}\pi\right) \\ &\quad \left. \cdot D_{-1}\left(\theta, \pi; \frac{3}{2}\pi\right) e^{-ika(\cos\theta - \cos\theta_0)/2} \right\} \\ &\cdot \sum_{s=1}^{\infty} \left(-\frac{1}{2}\right)^{2(s-1)} C\big((2s-1)ka\big) \\ &+ C(k\rho)\left\{ D_{-1}\left(\pi, \theta_0; \frac{3}{2}\pi\right) D_{-1}\left(\theta, \pi; \frac{3}{2}\pi\right) \right. \\ &\quad \cdot e^{-ika(\cos\theta + \cos\theta_0)/2} + D_{-1}\left(\frac{\pi}{2}, \frac{\pi}{2} + \theta_0; \frac{3}{2}\pi\right) \\ &\quad \left. \cdot D_{-1}\left(\frac{\pi}{2} + \theta, \frac{\pi}{2}; \frac{3}{2}\pi\right) e^{ika(\cos\theta + \cos\theta_0)/2} \right\} \\ &\cdot \sum_{t=1}^{\infty} \left(-\frac{1}{2}\right)^{2t-1} C(2tka). \end{aligned} \tag{8}$$

B. Modal Excitation

As depicted in Fig. 2, part of the primary edge-diffracted ray u_0 also propagates into slit Reg. 2) and is reradiated after several internal reflections and diffractions. On the basis of the assumption that the slit aperture is sufficiently wide compared with the wavelength, the total diffracted field can be formulated as a collection of internal reflected and diffracted rays. Inside the slit aperture [Reg. 2)], the ray description is unsuitable since an infinite number of multiply reflected rays exist owing to the waveguide structure, and the convergence of the ray summation is very slow. Accordingly, we apply a ray-mode conversion technique [17], [19] to obtain a rapid converging complementary parallel plane waveguide modal summation. The initial ray-mode conversion is performed at the upper end of the aperture ($x = \pm a/2,\ z = 0$) by extending the slit depth b to infinity. Then the modal summation $\dot{u}$ is given by

$$\dot{u} = \sum_{m=1}^{\infty} A_m U_m^- \tag{9}$$

where $U_m^{\pm}$ is the mth parallel plane waveguide mode

$$U_m^{\pm} = \sin\left\{\frac{m\pi}{a}\left(x + \frac{a}{2}\right)\right\}\exp(\pm i\zeta_m z) \tag{10}$$

and $\zeta_m = (k^2 - (m\pi/a)^2)^{1/2} = k\cos\theta_m$ is the modal propagation constant along the z-direction. A_m denotes the modal excitation coefficient for mode U_m^- as [19]

$$A_m = \frac{1}{2a\zeta_m}\left\{(-1)^m D_{-1}\left(\frac{3}{2}\pi - \theta_m, \theta_0; \frac{3}{2}\pi\right)e^{-ika(\cos\theta_0)/2} - D_{-1}\left(\theta_m, \theta_0 + \frac{\pi}{2}; \frac{3}{2}\pi\right)e^{ika(\cos\theta_0)/2}\right\}. \tag{11}$$

For $m < ka/\pi$, the mode propagates with the modal propagation angle

$$\theta_m = \sin^{-1}\left(\frac{m\pi}{ka}\right). \tag{12}$$

At $m = ka/\pi$, the mode U_m becomes cutoff and one obtains $\zeta_m = 0$. Then the coefficient A_m in (11) diverges. Accordingly, our solution fails to predict the correct field when the slit aperture width ka becomes close to a multiple of π. On the other hand, for $m > ka/\pi$, the propagation constant ζ_m along the z-direction becomes purely imaginary. Then the mode U_m becomes evanescent and decays exponentially as it propagates along the z-direction. Accordingly, the modal sum in (9) may be truncated at the final propagating mode $U_N^{\pm}$. However, if the slit thickness b is small, then the contribution from the evanescent modes cannot be ignored, as shown later. In order to find the evanescent modal excitation coefficient by the ray-mode conversion method, one needs to define the complex modal propagation angle $\hat{\theta}_m$ via analytic continuation into the complex angular domain. This is possible by defining $\hat{\theta}_m$ as

$$\hat{\theta}_m = \frac{\pi}{2} - i\cosh^{-1}\left(\frac{m\pi}{ka}\right). \tag{13}$$

It has already been found that the thus-derived excitation coefficient A_m in (11) is also valid for evanescent modes except near the cutoff frequency [23].

C. Modal Reradiation and Reflection Coupling

A mode U_m^- propagates toward the lower open end $z = -b$, at which modal radiation and reflection occur, as shown in Fig. 2. The modal radiation field u_1 in Reg. 3) can be formed by collecting all modal radiation fields generated by modes U_m^- at the lower aperture. At the same time, modal reflection occurs generating waveguide modes U_ℓ^+ propagating along the positive z-direction with new excitation coefficients. Note that modal coupling exists between different waveguide modes. Such modal reradiation and coupling can also be obtained by the high-frequency asymptotic method applied in [22]. The complex propagation angle $\hat{\theta}_m$ in (13) enables us to add the contribution from the nonpropagating evanescent modes, which may play an important role in the case of a narrow slit. It should be mentioned that each modal coupling element can be derived directly from the edge diffraction without solving the matrix equations to match the boundary condition. Accordingly, the calculation is very fast even for the case of a large aperture. One may also reduce the computational time by not using all the modes and selecting only the significant modes [17], [18].

D. Total Diffracted Field

The successive process of modal radiation and reflection/coupling continues to generate modal radiation fields u_{2n} in Reg. 1) ($z > 0$) and u_{2n+1} in Reg. 3) ($z < -b$). This modal radiation continues until all the energy of the bouncing waveguide modes is dissipated. Since a modal coupling occurs at every reflection process, the field description of modal reradiation may be complicated, although it can be written in a compact matrix form. The total of the radiation (diffraction) fields u_t in Reg. 1) can be given as

$$\begin{aligned} u_t^+ &= u_0 + \sum_{n=1}^{\infty} u_{2n} \\ &= u_0 + C(k\rho)[\boldsymbol{R}^+]\sum_{n=0}^{\infty}[\boldsymbol{B}]^{2n+1}[\boldsymbol{A}] \\ &= u_0 + C(k\rho)[\boldsymbol{R}^+][[\boldsymbol{I}] - [\boldsymbol{B}]^2]^{-1}[\boldsymbol{B}][\boldsymbol{A}] \end{aligned} \tag{14}$$

and in Reg. 3), it can be given as

$$\begin{aligned} u_t^- &= \sum_{n=0}^{\infty} u_{2n+1} \\ &= C(k\rho)[\boldsymbol{R}^-]\sum_{n=0}^{\infty}[\boldsymbol{B}]^{2n}[\boldsymbol{A}] \\ &= C(k\rho)[\boldsymbol{R}^-][[\boldsymbol{I}] - [\boldsymbol{B}]^2]^{-1}[\boldsymbol{A}]. \end{aligned} \tag{15}$$

In the above equations, $[\boldsymbol{R}^{\pm}]$ denotes the modal radiation row vector at the upper (+) and lower (−) aperture edges, and $[\boldsymbol{A}]$ is the modal excitation column vector due to the primary edge diffraction. Also, matrix $[\boldsymbol{B}]$ is the modal coupling matrix at each open end and $[\boldsymbol{I}]$ is a unit matrix. The components of the above matrices can be found in Appendix A. For these components, the effect of multiple edge diffraction between the upper and lower aperture edges can be determined and included. Thus, the sum of the multiply reflected modes at the

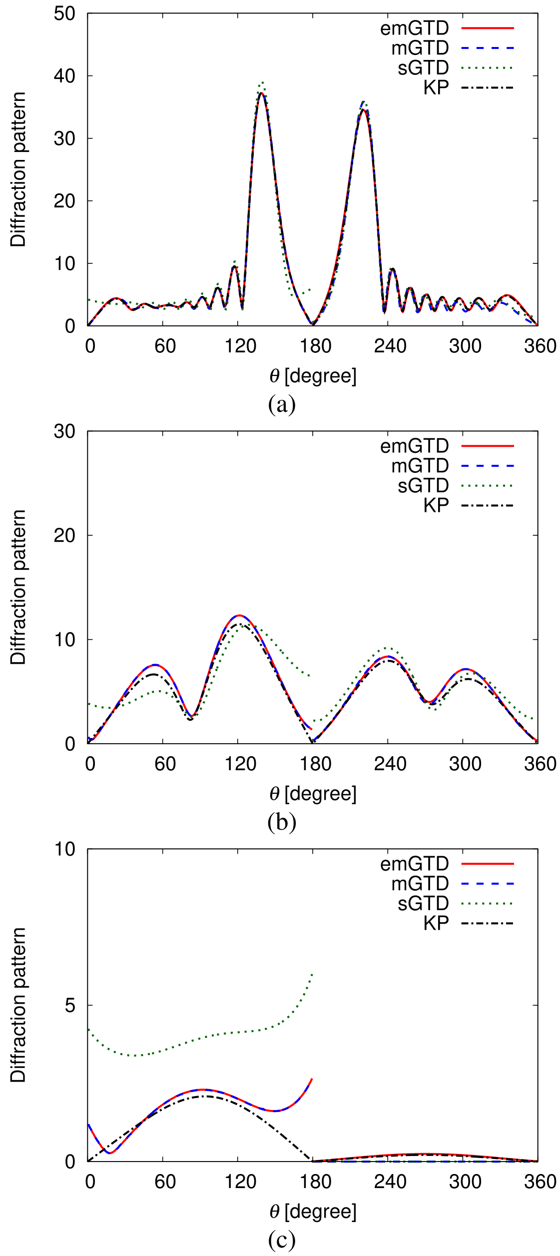

Fig. 3. Far-field diffraction patterns for $\theta_0 = 40°$ and $kb = 2$. (a) $ka = 30$. (b) $ka = 7$. (c) $ka = 2$. ——: present GTD results with the multiple edge interactions and the evanescent modal effect. – – –: GTD results with the multiple edge interactions. · · · ·: GTD results considering only the dominant edge-diffracted rays. – · – · –: KP method [8].

top and bottom open ends has a closed-form solution, as in (14) and (15), and one does not need to perform an actual summation, and the formulation should be valid, essentially regardless of the thickness b.

III. Numerical Results and Discussion

Let us now discuss the validity and accuracy of our formulation by comparing the numerical results with those obtained from another method. In Reg. 1), the reflected plane wave given by (2) exists but is omitted in the following calculation.

Fig. 3 shows the far-field diffraction patterns for different aperture widths. The common factor $C(k\rho)$ in (14) and (15) is omitted here. Three results calculated by our high-frequency

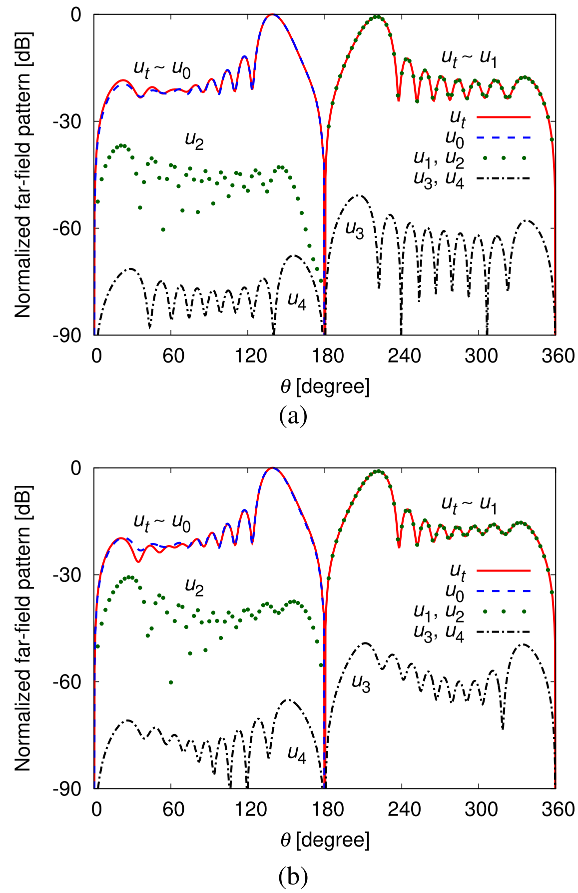

Fig. 4. Primary edge diffraction u_0 and modal reradiation contribution u_n ($n > 0$) for $\theta_0 = 40°$ and $ka = 30$. (a) $kb = 2$. (b) $kb = 4$. ——: total field. – – –: primary edge diffraction u_0 only. · · · ·: modal reradiation u_1, u_2. – · – · –: modal reradiation u_3, u_4.

asymptotic formulation are compared with the reference results obtained from the KP method [8], which is known to give reliable results for relatively narrow apertures. In these figures, the results estimated considering only dominant edge diffractions and propagation modes are denoted by sGTD, and those considering the effects of multiple edge diffraction such as in (8) are denoted by mGTD. Finally, the results considering multiple edge diffraction and evanescent modal effects are denoted by emGTD.

The plane wave incident angle θ_0 and slit thickness b are fixed as $\theta_0 = 40°$ and $kb = 2$, respectively, and three aperture widths, $ka = 30$, 7, and 2, are chosen as numerical examples. As expected, the contribution of the diffracted field decreases, as the slit aperture becomes narrower. One notices that the main lobe in Reg. 1) is tilted in close vicinity to the reflection boundary direction, and the number of diffraction lobes in Reg. 1) or 3) is closely related to the number of propagating parallel plane waveguide modes in Reg. 2). For the slit structure, the edge-diffracted rays such as $u_0^{\pm}$ in (3) are derived according to the local features of the aperture edges: thus they do not satisfy the boundary condition at the other side of the slit wall, on which the E_y component should be zero. Accordingly, the results obtained by sGTD do not vanish at $\theta = 0°$, 180°, and 360°. As can be seen in these figures, this deficiency can be mitigated by adding multiple

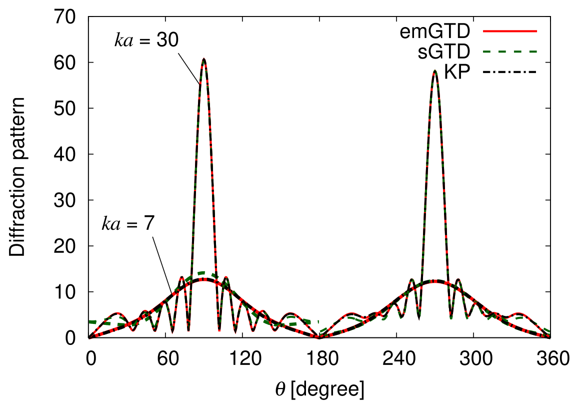

(a)

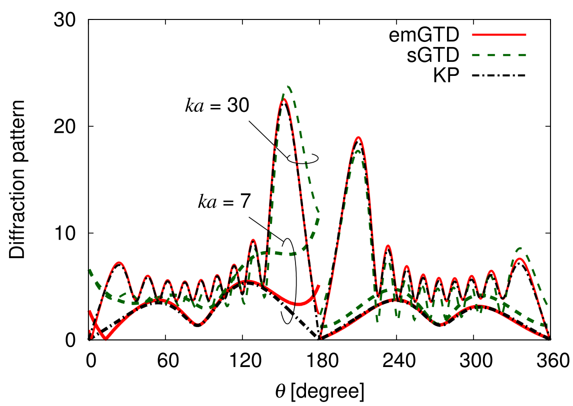

(b)

Fig. 5. Far-field diffraction patterns for $ka = 30$ and 7 and $kb = 2$. (a) $\theta_0 = 90°$. (b) $\theta_0 = 20°$. ——: present GTD results with multiple edge interactions and the evanescent modal effect. – – –: GTD results considering only the dominant edge-diffracted rays. – · – · –: KP method [8].

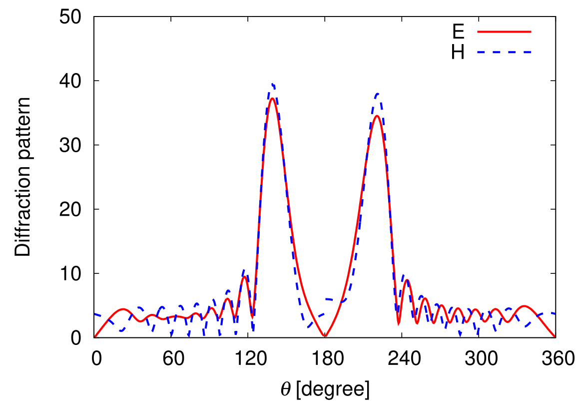

Fig. 6. Effect of difference in polarization for $\theta_0 = 40°$, $ka = 30$, and $kb = 2$. ——: present E-polarization. – – –: H-polarization [21].

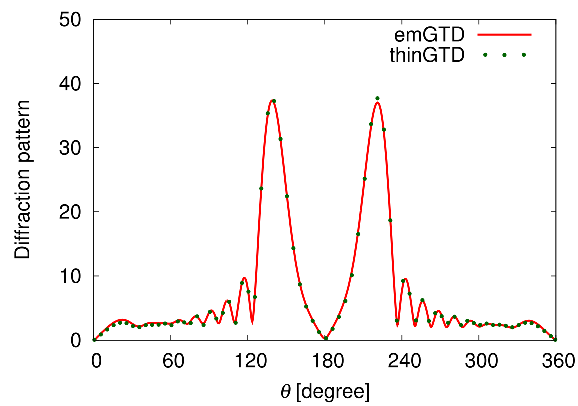

Fig. 7. Diffraction by an infinitely thin half-plane for $\theta_0 = 40°$ and $ka = 30$. ——: present GTD results ($b \to 0$) with the multiple edge interactions and the evanescent modal effect. · · · ·: GTD results for an infinitely thin slit ($b = 0$).

edge interaction terms, such as (8), except for the case of $ka = 2$ ($a = 0.32\ \lambda$) in Fig. 3(c), where the aperture may be too narrow to formulate with the high-frequency assumption. The effect of the evanescent modes appears to be insignificant but should not be ignored for diffraction in Reg. 3), even for the rather thick slit of $kb = 2$ ($b = 0.32\ \lambda$). Clearly, our emGTD results with two evanescent modes are in good agreement with the KP results in these figures. In particular, Fig. 3(c) shows the case when the slit is very narrow, no propagating parallel plane waveguide mode exists, and a weak diffracted wave is radiated in Reg. 3). It is noteworthy that our solution exactly matches the KP results for $180° < \theta < 360°$. Thus, our method can be used to estimate the electromagnetic wave leakage through a crack on a conducting wall.

Fig. 4 shows the contribution of individual diffracted rays u_n to the total field u_t. From this figure, one clearly sees that the primary edge-diffracted rays u_0 dominate in reflection Reg. 1), while the first modal radiation u_1 makes an important contribution in diffraction Reg. 3). Each successive modal radiation $u_n (n \geq 2)$ decays by roughly 15–20 dB for the slit depths $kb = 2$ and $kb = 4$ in Fig. 4(a) and (b), respectively. Thus, the decay mainly arises from the modal reflection coupling at the slit aperture ($z = 0, -b$).

Fig. 5(a) shows the diffraction patterns for the normal-incidence case $\theta_0 = 90°$. The patterns become symmetric with respect to the z-axis. Since the multiple edge-diffracted contributions are small for this incident angle, the pattern can be easily estimated by the dominant edge diffraction effect, denoted by sGTD. Fig. 5(b) shows the diffraction patterns for the grazing-incidence case $\theta_0 = 20°$. The contribution of diffraction is less than that in the normal-incidence case. It was found that our solutions become inaccurate in the vicinity of the screen. This is due to the fact that both incident and reflection shadow boundaries approach the aperture edge for the grazing-incidence case, the incident wave to the double edge diffraction becomes more involved, and the GTD results fail to predict the field properly.

The effect of a difference in polarization is shown in Fig. 6. The present E-polarization results are compared with those obtained previously for H-polarization [21]. Both results have almost the same main diffraction lobes, and a difference arises at the slit boundary direction owing to the difference in the boundary condition.

While the present formulation is based on a thick slit geometry with the slit aperture composed of four right-angle conducting wedges, it may be interesting to take the limit of $b \to 0$ to investigate the case of an infinitely thin slit. For this case, the diffraction pattern is known to be symmetric with respect to the screen [2]. Fig. 7 shows a comparison

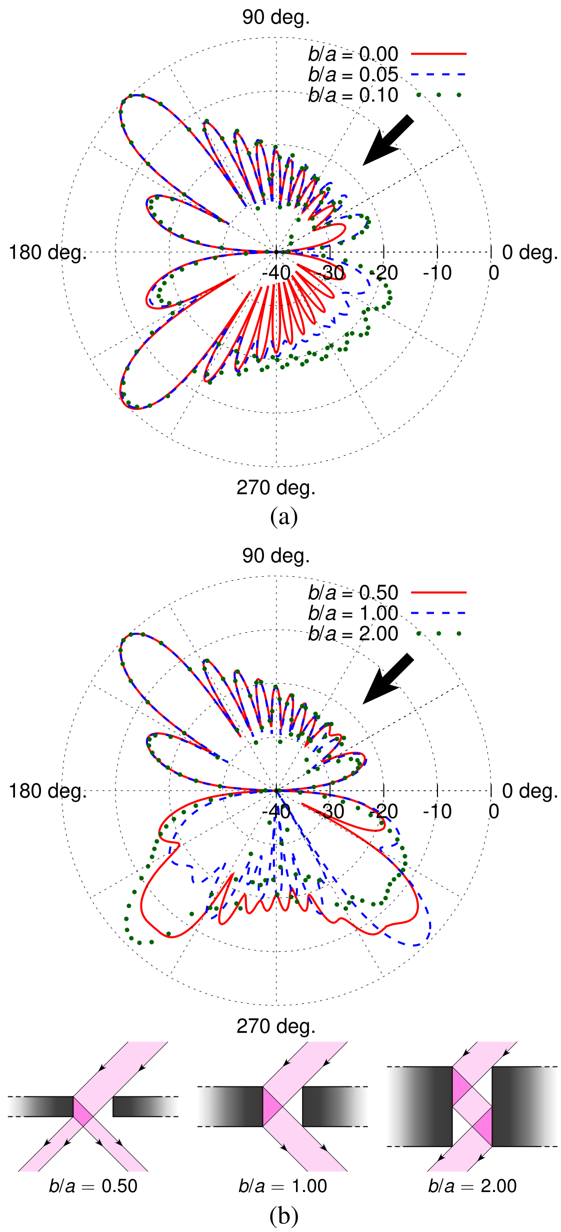

Fig. 8. Normalized diffraction pattern in decibel for various slit thicknesses $\theta_0 = 45°$ and $ka = 40$. (a) $b/a = 0.00$, 0.05, and 0.10. (b) $b/a = 0.50$, 1.00, and 2.00.

between our limiting case (emGTD) and the results for a slit on an infinitely thin screen (thinGTD). While our formulation gives us a different edge condition, our limiting results are in good agreement with those for an infinitely thin slit. An evanescent modal field is expected to play an important role for this limiting case.

Fig. 8 shows the change in the diffraction pattern with the screen thickness, In Reg. 1), primary edge-diffracted rays u_0 dominate and give the main diffraction pattern; thus, the pattern does not change essentially with the thickness. On the other hand, the pattern changes in the diffraction range [Reg. 3)]. When the screen is thin as in Fig. 8(a), the incident beam truncated by the aperture is mostly transmitted in the forward direction ($\theta = \theta_0 + \pi$) but scatters more in all directions than in the infinitely thin case. With increasing the thickness of the screen, the truncated beam undergoes reflection at the internal walls of the slit and the beam splits. For the incident angle $\theta_0 = 45°$ in Fig. 8(b), the almost equally split beam is radiated at $\theta = 225°$ and $315°$ for $b/a = 0.5$. For $b/a = 1.0$, all the truncated beam is reflected at the internal walls of the slit and is radiated at $\theta = 315°$, while the doubly bouncing beam is radiated at $\theta = 225°$ for $b/a = 2.0$. This observation can also be confirmed by the tracing geometrical optical beam.

IV. Conclusion

In this paper, E-polarized plane wave diffraction by a thick slit has been analyzed by a high-frequency asymptotic method. By including the evanescent modal effect inside the slit region as well as the multiple edge diffraction terms, our results are in good agreement with the reference results rigorously obtained by the KP method. This formulation can be used to estimate the transmission characteristics through building windows that are large compared with the wavelength. Since our solution is formulated by adding components that are excited successively along the propagation process, it gives us a better understanding with a physical interpretation of how electromagnetic waves propagate through a thick slit.

So far, our formulation has only been derived for empty apertures, and the effect of window glass is expected to be important and should be considered. This aspect is currently under study and will be reported in a separate paper.

Appendix
Modal Coupling Matrices

The components of the modal coupling matrices $[\boldsymbol{R}^+]$, $[\boldsymbol{R}^-]$, $[\boldsymbol{B}]$, and $[\boldsymbol{A}]$ in (14) and (15) are given as follows:

$$\begin{aligned}\{r^+_{1,p}\} = \frac{1}{2i}\Bigg\{&(-1)^p D_{-1}\left(\theta, \frac{3}{2}\pi - \theta_p; \frac{3}{2}\pi\right) e^{-ika(\cos\theta)/2} \\ &- D_{-1}\left(\theta + \frac{\pi}{2}, \theta_p; \frac{3}{2}\pi\right) e^{ika(\cos\theta)/2}\Bigg\} \\ &+\frac{1}{2i}\Bigg[\Bigg\{(-1)^p D_{-1}\left(\pi, \frac{3}{2}\pi - \theta_p; \frac{3}{2}\pi\right) \\ &\cdot D_{-1}\left(\theta + \frac{\pi}{2}, \frac{\pi}{2}; \frac{3}{2}\pi\right) e^{ika(\cos\theta)/2} \\ &- D_{-1}\left(\frac{\pi}{2}, \theta_p; \frac{3}{2}\pi\right) D_{-1}\left(\theta, \pi, \frac{3}{2}\pi\right) \\ &\cdot e^{-ika(\cos\theta)/2}\Bigg\} \\ &\cdot \sum_{s=1}^{\infty}\left(-\frac{1}{2}\right)^{2(s-1)} C((2s-1)ka) \\ &+\Bigg\{(-1)^p D_{-1}\left(\pi, \frac{3}{2}\pi - \theta_p; \frac{3}{2}\pi\right) \\ &\times D_{-1}\left(\theta, \pi; \frac{3}{2}\pi\right) \cdot e^{-ika(\cos\theta)/2} \\ &- D_{-1}\left(\frac{\pi}{2}, \theta_p; \frac{3}{2}\pi\right) \cdot D_{-1}\left(\theta + \frac{\pi}{2}, \frac{\pi}{2}; \frac{3}{2}\pi\right) \\ &\times e^{ika(\cos\theta)/2}\Bigg\} \cdot \sum_{t=1}^{\infty}\left(-\frac{1}{2}\right)^{2t-1} C(2tka)\Bigg]\end{aligned} \tag{16}$$

$$\begin{aligned}\{r_{1,p}^{-}\} &= \frac{1}{2i}\left\{(-1)^p D_{-1}\left(\theta-\frac{\pi}{2},\theta_p,\frac{3}{2}\pi\right)e^{-ik\ddot{\rho}\cos(\theta+\ddot{\theta})}\right.\\ &\quad\left.-D_{-1}\left(\theta-\pi,\frac{3}{2}\pi-\theta_p;\frac{3}{2}\pi\right)e^{ik\ddot{\rho}\cos(\theta-\ddot{\theta})}\right\}\\ &\quad+\frac{1}{2i}\left[\left\{(-1)^p D_{-1}\left(\frac{\pi}{2},\theta_p;\frac{3}{2}\pi\right)\right.\right.\\ &\quad\cdot D_{-1}\left(\theta-\pi,\pi;\frac{3}{2}\pi\right)e^{ik\ddot{\rho}\cos(\theta-\ddot{\theta})}\\ &\quad-D_{-1}\left(\pi,\frac{3}{2}\pi-\theta_p;\frac{3}{2}\pi\right)D_{-1}\\ &\quad\left.\times\left(\theta-\frac{\pi}{2},\frac{\pi}{2};\frac{3}{2}\pi\right)\cdot e^{-ik\ddot{\rho}\cos(\theta+\ddot{\theta})}\right\}\\ &\quad\cdot\sum_{s=1}^{\infty}\left(-\frac{1}{2}\right)^{2(s-1)}C((2s-1)ka)\\ &\quad+\left\{(-1)^p D_{-1}\left(\frac{\pi}{2},\theta_p;\frac{3}{2}\pi\right)D_{-1}\left(\theta-\frac{\pi}{2},\frac{\pi}{2};\frac{3}{2}\pi\right)\right.\\ &\quad\cdot e^{-ik\ddot{\rho}\cos(\theta+\ddot{\theta})}-D_{-1}\left(\pi,\frac{3}{2}\pi-\theta_p;\frac{3}{2}\pi\right)\\ &\quad\left.\cdot D_{-1}\left(\theta-\pi,\pi;\frac{3}{2}\pi\right)e^{ik\ddot{\rho}\cos(\theta-\ddot{\theta})}\right\}\\ &\quad\left.\cdot\sum_{t=1}^{\infty}\left(-\frac{1}{2}\right)^{2t-1}C(2tka)\right]\end{aligned}\tag{17}$$

$$\begin{aligned}\{b_{p,q}\} &= \frac{1}{4a\zeta_p i}e^{i\zeta_p b}D_{-1}\left(\theta_p,\theta_q;\frac{3}{2}\pi\right)\{(-1)^{p+q}+1\}\\ &\quad+\frac{1}{4a\zeta_p i}e^{i\zeta_p b}D_{-1}\left(\frac{\pi}{2},\theta_q;\frac{3}{2}\pi\right)D_{-1}\left(\theta_p,\frac{\pi}{2};\frac{3}{2}\pi\right)\\ &\quad\cdot\left[\{(-1)^{p+1}+(-1)^{q+1}\}\right.\\ &\quad\cdot\sum_{s=1}^{\infty}\left(-\frac{1}{2}\right)^{2(s-1)}C((2s-1)ka)\\ &\quad\left.+\{(-1)^{p+q}+1\}\cdot\sum_{t=1}^{\infty}\left(-\frac{1}{2}\right)^{2t-1}C(2tka)\right]\end{aligned}\tag{18}$$

$$\begin{aligned}\{a_{q,1}\} &= \frac{1}{2a\zeta_q}e^{i\zeta_q b}\\ &\quad\cdot\left\{(-1)^q D_{-1}\left(\frac{3}{2}\pi-\theta_q,\theta_0;\frac{3}{2}\pi\right)e^{-ika(\cos\theta_0)/2}\right.\\ &\quad\left.-D_{-1}\left(\theta_q,\theta_0+\frac{\pi}{2};\frac{3}{2}\pi\right)e^{ika(\cos\theta_0)/2}\right\}+\frac{1}{2a\zeta_q}e^{i\zeta_q b}\\ &\quad\times\left[\left\{(-1)^q D_{-1}\left(\frac{\pi}{2},\theta_0+\frac{\pi}{2};\frac{3}{2}\pi\right)\right.\right.\\ &\quad\cdot D_{-1}\left(\frac{3}{2}\pi-\theta_q,\pi;\frac{3}{2}\pi\right)e^{ika(\cos\theta_0)/2}\\ &\quad-D_{-1}\left(\pi,\theta_0;\frac{3}{2}\pi\right)D_{-1}\left(\theta_q,\frac{\pi}{2};\frac{3}{2}\pi\right)\\ &\quad\left.\cdot e^{-ika(\cos\theta_0)/2}\right\}\cdot\sum_{s=1}^{\infty}\left(-\frac{1}{2}\right)^{2(s-1)}C((2s-1)ka)\\ &\quad+\left\{(-1)^q D_{-1}\left(\pi,\theta_0;\frac{3}{2}\pi\right)\right.\\ &\quad\times D_{-1}\left(\frac{3}{2}\pi-\theta_q,\pi;\frac{3}{2}\pi\right)\cdot e^{-ika(\cos\theta_0)/2}\\ &\quad-D_{-1}\left(\frac{\pi}{2},\theta_0+\frac{\pi}{2};\frac{3}{2}\pi\right)\\ &\quad\left.\cdot D_{-1}\left(\theta_q,\frac{\pi}{2};\frac{3}{2}\pi\right)e^{ika(\cos\theta_0)/2}\right\}\\ &\quad\left.\cdot\sum_{t=1}^{\infty}\left(-\frac{1}{2}\right)^{2t-1}C(2tka)\right]\end{aligned}\tag{19}$$

where integers p, q $(= 1, 2, 3, \ldots)$ are modal numbers, $\ddot{\rho} = ((a/2)^2 + b^2)^{1/2}$, and $\ddot{\theta} = \tan^{-1}(2b/a)$. Other symbols correspond to those in (11) and (12). Note that the above results are derived on a high-frequency base, and should be valid for $ka \gg 1$, except at specific modal cutoff frequencies.

REFERENCES

[1] P. M. Morse and P. J. Rubenstein, "The diffraction of waves by ribbons and by slits," *Phys. Rev.*, vol. 54, no. 11, pp. 895–898, 1938.

[2] S. N. Karp and A. Russek, "Diffraction by a wide slit," *J. Appl. Phys.*, vol. 27, no. 8, pp. 886–894, Aug. 1956.

[3] Y. Nomura and S. Katsura, "Diffraction of electromagnetic waves by ribbon and slit. I," *J. Phys. Soc. Jpn.*, vol. 12, no. 2, pp. 190–200, 1957.

[4] J. J. Bowman, T. B. A. Senior, and P. L. E. Uslenghi, Eds., *Electromagnetic and Acoustic Scattering by Simple Shapes*. New York, NY, USA: Hemisphere, 1969.

[5] I. Kobayashi, "Darstellung eines Potentials in zylindrischen Koordinaten, das sich auf einer Ebene innerhalb und ausserhalb einer gewissen Kreisbegrenzung verschi edener Grenzbedingung unterwirft," (in German), *Sci. Rep. Tohoku Imp. Univ.*, vol. 20, no. 1, pp. 197–212, 1931.

[6] J. B. Keller, "Geometrical theory of diffraction," *J. Opt. Soc. Amer.*, vol. 52, no. 2, pp. 116–130, Feb. 1962.

[7] K. Hongo, "Diffraction of electromagnetic plane wave by infinite slit perforated in a conducting screen with finite thickness," (in Japanese), *Trans. IECE*, vol. 54-B, no. 7, pp. 419–425, Jul. 1971.

[8] K. Hongo and G. Ishii, "Diffraction of an electromagnetic plane wave by a thick slit," *IEEE Trans. Antennas Propag.*, vol. 26, no. 3, pp. 494–499, May 1978.

[9] S. Kashyap and M. A. K. Hamid, "Diffraction characteristics of a slit in a thick conducting screen," *IEEE Trans. Antennas Propag.*, vol. 19, no. 4, pp. 499–507, Jul. 1971.

[10] S. C. Kashyap, M. A. K. Hamid, and N. J. Mostowy, "Diffraction pattern of a slit in a thick conducting screen," *J. Appl. Phys.*, vol. 42, no. 2, pp. 894–895, 1971.

[11] N. Morita, "Diffraction of electromagnetic wave by a two-dimensional aperture with arbitrary cross section shape," (in Japanese), *Trans. IECE*, vol. 54-B, no. 5, pp. 218–222, May 1971.

[12] F. L. Neerhoff and G. Mur, "Diffraction of a plane electromagnetic wave by a slit in a thick screen placed between two different media," *Appl. Sci. Res.*, vol. 28, pp. 73–88, Jul. 1973.

[13] S. H. Kang, H. J. Eom, and T. J. Park, "TM scattering from a slit in a thick conducting screen: Revisited," *IEEE Trans. Microw. Theory Techn.*, vol. 41, no. 5, pp. 895–899, May 1993.

[14] T. J. Park, S. H. Kang, and H. J. Eom, "TE scattering from a slit in a thick conducting screen: Revisited," *IEEE Trans. Antennas Propag.*, vol. 42, no. 1, pp. 112–114, Jan. 1994.

[15] L. B. Felsen, "Progressing and oscillatory waves for hybrid synthesis of source excited propagation and diffraction," *IEEE Trans. Antennas Propag.*, vol. 32, no. 8, pp. 775–796, Aug. 1984.

[16] P. H. Pathak and R. J. Burkholder, "Modal, ray, and beam techniques for analyzing the EM scattering by open-ended waveguide cavities," *IEEE Trans. Antennas Propag.*, vol. 37, no. 5, pp. 635–647, May 1989.

[17] H. Shirai and L. B. Felsen, "Rays, modes and beams for plane wave coupling into a wide open-ended parallel-plane waveguide," *Wave Motion*, vol. 9, no. 4, pp. 301–317, Jul. 1987.

[18] A. Altintas, P. H. Pathak, and M.-C. Liang, "A selective modal scheme for the analysis of EM coupling into or radiation from large open-ended waveguides," *IEEE Trans. Antennas Propag.*, vol. 36, no. 1, pp. 84–96, Jan. 1988.

[19] H. Shirai and K. Hirayama, "Ray mode coupling analysis of plane wave scattering by a trough," *IEICE Trans. Commun.*, vol. E76-B, no. 12, pp. 1558–1563, Dec. 1993.

[20] H. Shirai, "Ray mode coupling analysis of EM wave scattering by a partially filled trough," *J. Electromagn. Waves Appl.*, vol. 8, no. 11, pp. 1443–1464, Nov. 1994.

[21] H. Shirai and R. Sato, "High frequency ray-mode coupling analysis of plane wave diffraction by a wide and thick slit on a conducting screen," *IEICE Trans. Electron.*, vol. E95-C, no. 1, pp. 10–15, Jan. 2012.

[22] H. Y. Yee, L. B. Felsen, and J. B. Keller, "Ray theory of reflection from the open end of a waveguide," *SIAM J. Appl. Math.*, vol. 16, no. 2, pp. 268–300, Mar. 1968.

[23] H. Shirai, Y. Matsuda, and R. Sato, "GTD analysis for evanescent modal excitation," *IEICE Trans. Electron.*, vol. E80-C, no. 1, pp. 190–192, Jan. 1997.

Hiroshi Shirai received the B.E. and M.E. degrees in electrical engineering from Shizuoka University, Shizuoka, Japan, in 1980 and 1982, respectively, and the Ph.D. degree from Polytechnic University (currently renamed as New York University, Tandon School of Engineering), New York City, NY, USA, in 1986.

He was initially a Research Fellow, then a Post-Doctoral Scientist until 1987 at Polytechnic University. Since 1987, he has been with Chuo University, Tokyo, Japan, where he is currently a Professor. His current research interests include wave propagation and diffraction in time harmonic and transient domains.

Dr. Shirai is a fellow of IEICE and the Electromagnetic Academy, and a member of Sigma Xi and the Institute of Electrical Engineers of Japan. He was a recipient of the R. W. P. King Best Paper Award from the Antennas and Propagation Society of the IEEE in 1987. He has been serving as a Committee Member of various technical societies and international meetings. He is now an Editorial Advisory Member of Fundamentals Review of the Institute of Electronics, Information and Communication Engineers.

Masayuki Shimizu received the B.E. degree in electrical, electronic, and communication engineering from the Faculty of Science and Engineering, Chuo University, Tokyo, Japan, in 2015, where he is currently pursuing the M.E. degree in electrical, electronic, and communication engineering.

His current research interests include electromagnetic wave scattering.

Ryoichi Sato received the B.S., M.S., and Ph.D. degrees in electrical engineering from Chuo University, Tokyo, Japan, in 1992, 1994, and 1997, respectively.

Since 1997, he has been with the Faculty of Education (Faculty of Education and Human Sciences), Niigata University, Niigata, Japan, where he is currently a Professor. In 2002, he was a Research Scholar at the New York University Tandon School of Engineering, Brooklyn, NY, USA. His current research interests include electromagnetic wave propagation, scattering and diffraction, and radar polarimetry.

Dr. Sato is a member of the Institute of Electronics, Information and Communication Engineers of Japan, and the Institute of Electrical Engineers of Japan. He was a recipient of the Young Scientist Paper Award of the 5th International Conference on Mathematical Methods in Electromagnetic Theory in 1994, the Paper Presentation Award from the Institute of Electrical Engineers of Japan in 2000, and the Best Poster Award of the 7th European Conference on Synthetic Aperture Radar in 2008.